NORDIC STEEL 2024
The 15th Nordic Steel Construction Conference,
June 26–28, 2024, Luleå, Sweden

Ultra-high strength fillet- and butt-welded joints made of S960

Load-carrying capacity and deformation behaviour

Mareike von Arnim*[,a], Stefan Eichler[b], Oliver Brätz[c], Ulrike Kuhlmann[a], Jörg Hildebrand[b], Jean Pierre Bergmann[b], Wilko Flügge[c]

[a]University of Stuttgart, Institute of Structural Design, Germany
mareike.von-arnim@ke.uni-stuttgart.de, ulrike.kuhlmann@ke.uni-stuttgart.de
[b]TU Ilmenau, Department of Mechanical Engineering, Production Technology Group, Germany
stefan.eichler@tu-ilmenau.de, joerg.hildebrand@tu-ilmenau.de, jeanpierre.bergmann@tu-ilmenau.de
[c]Fraunhofer Institute for Large Structures in Production Engineering IGP, Rostock, Germany
oliver.braetz@igp.fraunhofer.de, wilko.fluegge@igp.fraunhofer.de

ABSTRACT

High and ultra-high strength steel can contribute to more sustainable structures by saving construction weight and resources. In FprEN 1993-1-8 modified design rules for butt- und fillet-welded connections have been implemented for steels up to S700 that consider the special characteristics of welded high-strength steels. prEN 1993-1-12 will be valid for steels up to S960 and consequently, the design concepts have to be extended up to S960. For this purpose, in the research project “Effective design concepts for mixed connections in steel structures” an extensive experimental program of ultra-high strength welded connections was tested. For butt welds, 36 specimens with steel grades S960MC or S960QL and different filler metals G46 and G89 were used. Furthermore, the plate thickness and weld joint geometry were varying parameters. The fillet welds were made of S960QL, $t = 20$ mm with varying filler metals G46, G69, G89 and T89, resulting in a total of 12 experimental tests. Tensile tests with optical strain and optical extensometer measuring were conducted to examine the load-carrying capacity and deformation behaviour of the welded test specimens. Moreover, further material investigations were carried out, such as microhardness mappings on in cross-sectioned welds and tensile tests of the weld metal. With the results obtained from the research project, proposals for extensions of the design concepts for butt- and fillet-welded connections up to S960 were developed that can be incorporated in prEN 1993-1-12. The investigations carried out and the formulation of design recommendations enable a wide use of ultra-high strength steels. This allows material savings and future-oriented, sustainable constructions.

Keywords: Ultra-high strength steel (UHSS), butt welds, fillet welds, S960

1 INTRODUCTION

Continuous further development is leading to even higher strength steels, with the result that S960 steels have been available on the market for years. For the use of ultra-high strength steels (UHSS) in the construction industry, such as buildings or steel bridges, their incorporation into European standards is of great importance. Hence, in the new generation of Eurocode 3, there is a whole new part 1-12 (1) that addresses steels S700 < S ≤ S960. For this purpose, extensive investigations must be carried out in order to extend or adapt design concepts up to S960. Therefore, as part of the research project “Effective design concepts for mixed connections” (2) investigations were conducted on butt welds and fillet welds made of S960. The results obtained and the design proposals derived are presented here.

The conducted research is essential to enable user-friendly applications of high-strength steels. This allows slender and resource-efficient constructions that contribute to a sustainable development due to the reduced construction weight.
Within the scope of the research project, further investigations were carried out on butt welds as mixed joints of different steels and on butt welds made of thin sheets with t = 3 mm, as described in (3), (4).

2 STATE OF THE ART

Welding high-strength steel (HSS) and UHSS can lead to a formation of a soft zone in the heat-affected zone (HAZ), showing hardness reductions of over 20 % compared to the unaltered base metal (5), (6), (7). This can cause a premature failure in the HAZ with reduced load-carrying capacity of butt-welded joints. Consequently, it was necessary to develop a new design concept in order to be able to safely design butt welds of HSS. For this, *Eq. (1)* was developed, that is included in FprEN 1993-1-8 (8).

$$\sigma_{\mathrm{v,Rd}} = \frac{0{,}85\ (0{,}9 f_{\mathrm{u}}) + 0{,}15 f_{\mathrm{u,FM}}}{\gamma_{\mathrm{M2}}} \tag{1}$$

with:
f_{u} = tensile strength of base metal
$f_{\mathrm{u,FM}}$ = tensile strength of filler material according to FprEN 1993-1-8, Table 6.2 (8)
γ_{M2} = partial factor (= 1,25)

The factor 0,9 considers the possible softening effect in the HSS's and UHSS's HAZ due to welding. Furthermore, *Eq. (1)* allows for the use of filler materials of lower (undermatching), equal (matching) or higher (overmatching) tensile strength than the connected base metal. This allows the load-carrying capacity of butt welds to be specifically increased, for example with the selective use of an overmatching filler material. For matching butt welds, *Eq. (1)* is valid for S460 < S ≤ S700 and for overmatching and undermatching filler materials it is valid for steels S460 ≤ S ≤ S700.
As part of the revision to FprEN 1993-1-8 (8), the design concept for fillet welds was expanded and a new concept was introduced into the standardisation. For fillet welds with matching weld consumable, the load-carrying capacity is calculated by *Eq. (2)*. New correlation coefficients β_{w} were developed up to S700 for this purpose, see FprEN 1993-1-8, Table 6.1 (8).

$$\sqrt{\sigma_{\perp}^2 + 3(\tau_{\perp}^2 + \tau_{\parallel}^2)} \leq \frac{f_u}{\beta_w \gamma_{M2}} \quad \text{and} \quad \sigma_{\perp} \leq \frac{0{,}9 f_u}{\gamma_{M2}} \tag{2}$$

with:
β_{w} = correlation coefficients according to FprEN 1993-1-8, Table 6.1 (8)

The new equation from FprEN 1993-1-8 (8), see *Eq. (3)*, increases the application range of high-strength fillet welds made of S460 ≤ S ≤ S700, as it is also possible to design welds with undermatching or overmatching filler materials. As can be seen from the weighting of 75 % $f_{\mathrm{u,FM}}$ in *Eq. (3)*, the load-carrying capacity of fillet welds largely depends on the filler material used. This is further underlined by the modified correlation coefficient $\beta_{\mathrm{w,mod}}$, see FprEN 1993-1-8, Table 6.2 (8), that is also selected based on the filler material used in the welded joint.

$$\sqrt{\sigma_{\perp}^2 + 3(\tau_{\perp}^2 + \tau_{\parallel}^2)} \leq \frac{0{,}25 f_{\mathrm{u}} + 0{,}75 f_{\mathrm{u,FM}}}{\beta_{w,mod} \gamma_{\mathrm{M2}}} \quad \text{and} \quad \sigma_{\perp} \leq \frac{0{,}9 f_u}{\gamma_{M2}} \tag{3}$$

with:
$\beta_{\mathrm{w,mod}}$ = modified correlation coefficients according to FprEN 1993-1-8, Table 6.2 (8)

The design concepts for welded joints presented in *Eq. (1)-(3)* are all valid for steels up to S700 and they are included in FprEN 1993-1-8 (8). For the new part prEN1993-1-12 (1), investigations are required in order to extend and adapt the design concepts up to S960. They were carried out within the scope of (2) and the results and design proposals for welded joint made out of S700 < S ≤ S960 are presented as follows.

3 EXPERIMENTAL INVESTIGATIONS

3.1 Materials and manufacturing

A total of 36 tests of butt welds and twelve tests of longitudinal fillet welds were manufactured and tested. Two UHSS grades and four different welding consumables were used. The base metals and filler materials used, with their corresponding actual material properties according to the acceptance test certificate are given in *Table 1*.

Table 1. Base metals and filler materials with actual material properties

Material	**Specification**	**Dimension**	R_{eH} **or** $R_{p0,2}$ in MPa	R_m in MPa
S960QL	EN 10025-6-S960QL (1.8933)	t = 10 mm	1036	1077
		t = 20 mm	1045	1074
S960MC	EN 10149-2-S960MC (1.8799)	t = 10 mm	965	1022
G46	ISO 14341-A G 46 5 M21 4Si1	Ø 1,2 mm	525	598
G69	ISO 16834-A G 69 6 M21 Mn4Ni1.5CrMo	Ø 1,2 mm	761	806
G89	ISO 16834-A G 89 6 M21 Mn4Ni2CrMo	Ø 1,2 mm	1040	1108
T89	ISO 18276-A T 89 4 Z M M21 3 H5	Ø 1,2 mm	931	993

The steels S960QL in t = 10 and 20 mm and S960MC in t = 10 mm were used for butt welds, that were welded with G46 and G89 filler materials, respectively. G46 is an undermatching welding consumable and G89 can be classified as matching here, as can be seen from the tensile strengths in *Table 1*, since $R_{m,G89} \geq R_{m,S960}$. Furthermore, the test specimens were manufactured as single-V and double-V groove, to examine the influence of the weld joint geometry. The heat input during welding was determined by the cooling time $t_{8/5}$ and was selected as high for the materials used. This leads to a greater thermal impact and soft zone formation in the HAZ and is therefore on the safe side in order to develop design concepts (9) (10). Three test specimens were produced from each configuration, resulting in a total of 36 butt welds being tested. The test specimens for fillet welds were manufactured with S960QL, t = 20 mm using the filler materials G46, G69, T89 and G89. Hereby, also three test specimens were welded for each combination, making a total of twelve fillet welds.

The manufacturing process of the welded test specimens is shown in *Fig. 1*. Further information and explanations on welding of the test specimens, including details about the cooling time $t_{8/5}$, can be found in (11).

The geometric measures of the welded test specimens are given in *Fig. 2*. For the butt welds, a geometry according to EN ISO 6892-1 (12) is used. The length of the tested longitudinal fillet welds were 50 mm each and they were precisely defined by milled grooves. The nominal fillet weld throat thickness for production was specified as a = 4 mm.

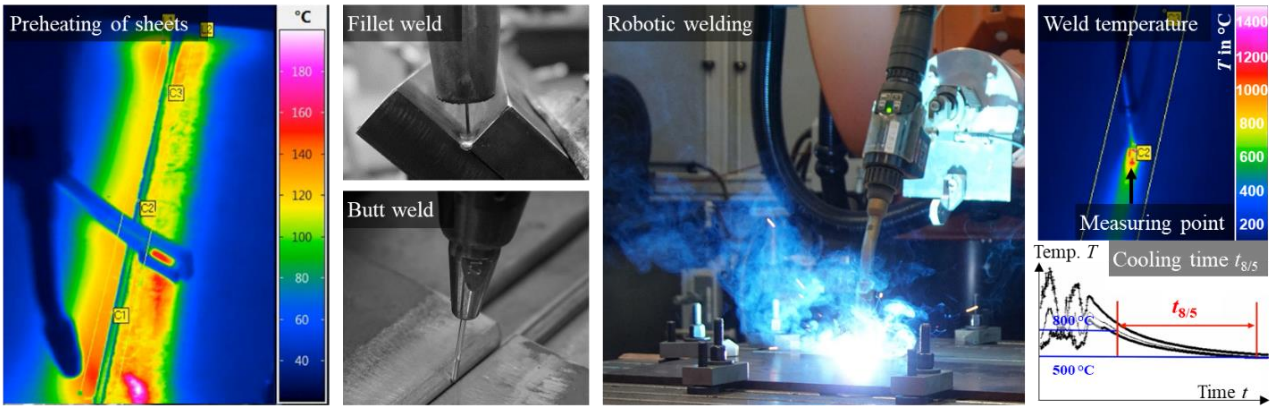

Fig. 1. Manufacturing of welded test specimens, incl. verification of inductive preheating and determination of cooling times

a)

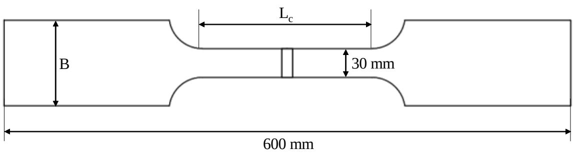

B = 60 mm for t = 10 mm
= 90 mm for t = 20 mm
L_c = 130 mm for t = 10 mm
= 180 mm for t = 20 mm

b)

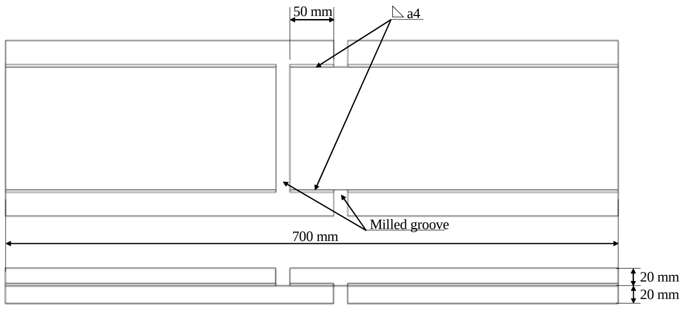

Fig. 2. Geomety of welded test specimens a) butt weld and b) longitudinal fillet weld

3.2 Experimental procedure

The experimental tests were conducted as quasi-static tensile tests, displacement-controlled until failure of the specimens. This involved measuring the test force with the integrated load cell, displacements and strains were measured using DIC (Digital Image Correlation) with ARAMIS. One ARAMIS-measuring system was used for the butt welds and two coupled systems were used for the fillet welds in order to measure both fillet welds during the execution of the tests. The test setup for butt welds is given in *Fig. 3*.

In order to calculate the maximum stress achieved by the butt-welded test specimens, the maximum test force reached is divided by the initial cross-section at the location of failure. The cross-section of the weld seam in fillet welds cannot be measured precisely before failure of the sample. Therefore, the failed samples were 3D scanned here. This allowed the fracture surface to be determined, also considering the deep penetration of the fillet weld. The maximum test force is divided by the fracture surface of the two fillet

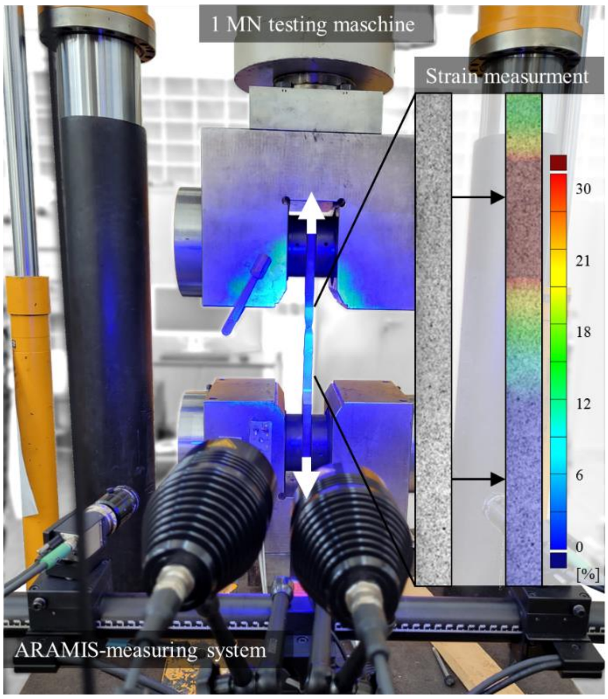

Fig. 3. Experimental test set-up for transverse tensile testing of butt welds

welds of each sample to obtain the maximum stress for the fillet welds.
Extensive further investigations were carried out, including tensile tests on the weld metal with varying cooling time $t_{8/5}$ and hardness mappings with the UCI method (Ultrasonic Contact Impedance), as defined in standards ASTM A1038 (13) and DIN 50159-1 (14), on the weld seams. Comparative measurements were carried out to validate the UCI hardness mappings confirming good agreement with deviations in the standard range (15). The influencing factors of the welded joints were analysed in greater depth with these further investigations.

4 EXPERIMENTAL RESULTS AND DISCUSSION

4.1 Butt welds

The load-carrying capacity of welded butt joints made of S960 is shown in *Fig. 4*. Here, the results are displayed dependent on the varying parameters weld seam preparation, filler material and failure location. In addition, a normalized stress diagram was selected. For this purpose, the maximum stress is divided by the tensile strength of the steel used in order to easily compare the results from different steel grades.
Failure of the specimens occurred in the filler material (FM), HAZ or base metal (BM). All undermatching joints with G46 showed a failure in the weld metal. This behaviour can be explained by the significantly lower tensile strength of G46 compared to S960, that is also visible in the hardness mappings, see *Fig. 5*. Furthermore, a double-V weld resulted in average in an increased load-carrying capacity of 9 % compared to a single-V weld for the undermatching connections. This is due to the larger weld metal volume of the V-weld, as well as the slightly lower hardness values in the V-weld, that is visible in *Fig. 5*. The deformation behaviour just before failure is shown in *Fig. 6a)* for an undermatching joint with double-V weld.
For the matching butt welds, the failure occurred either in the HAZ or in the unaltered base metal. There is a slight indication that single-V welds failed more frequently in the HAZ compared to double-V welds. On the one hand, this may be caused by the failure angle that can form more easily along the HAZ in the single-V configuration than in the double-V one. On the other hand, the double-V weld also forms a smaller soft zone having a positive effect on the overall load-carrying capacity. Ten out of the 18 matching test specimens failed in the HAZ with an average load-carrying reduction of 3 % compared to the tensile strength of the base metal. *Fig. 6* shows the

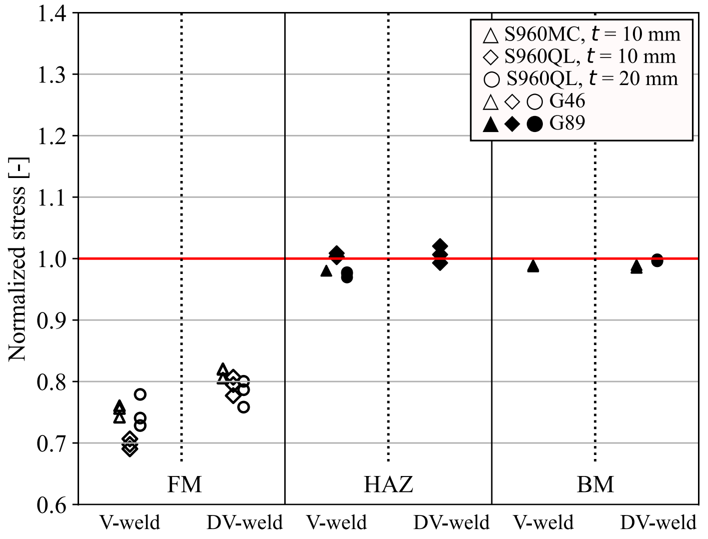

Fig. 4. Experimental results of ultra-high strength butt welds dependent on the filler material, weld preparation and location of failure

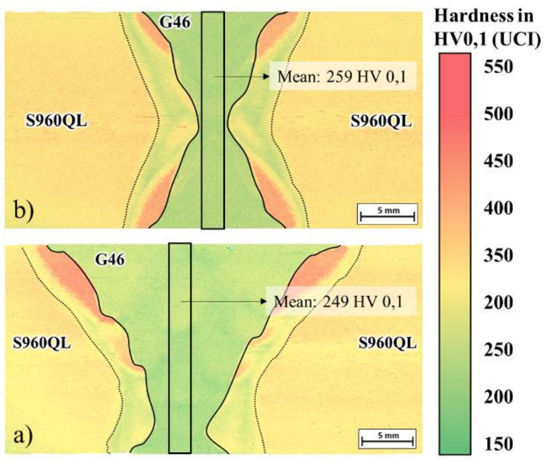

Fig.5. Hardness mappings with UCI method, S960QL, t = 20 mm: a) V-weld with G46, b) DV-weld with G46

deformation behaviour before failure of the specimens, while in *Fig. 6b)* the failure appeared in the HAZ and in *c)* the failure appeared in the base material. In case of failure in the base material, a small strain concentration is also evident in the HAZ.

An additional observation was that failure in the weld metal or in the HAZ leads to lower deformations in the connections compared to failure in the base metal. This is based on the significantly reduced cross-section, especially in the HAZ, where the strains are distributed compared to a base metal failure.

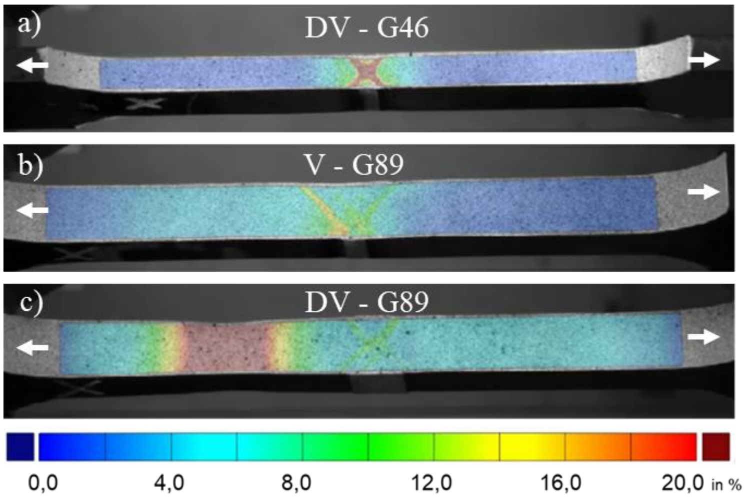

Fig.6. Deformation behaviour with ARAMIS for a) 10 mm specimen S960 with G46 and DV-weld, b) 20 mm specimen S960 with G89 and V-weld, c) 20 mm specimen S960 with G89 and DV-weld

No significant influence on the load-carrying capacity was found between the tested plate thicknesses $t = 10$ or 20 mm and the different steel grades S960QL and S960MC.

4.2 Fillet welds

A total of twelve tests were carried out on fillet welds using four different welding consumables. As explained in section 3.2, the actual fracture surface, that was determined using a 3D scan, was used to calculate the maximum stresses achieved. The effective throat thickness including a deep penetration was thus determined to be 7,4 mm on average compared to nominal $a = 4$ mm. The deep penetration is also clearly visible in the hardness mappings in *Fig. 9*. The evaluation of the ARAMIS examinations of both fillet welds showed that the failure occurred simultaneously in both fillet welds in ten out of twelve cases. Both fracture surfaces were therefore used to obtain the stress for each experimental test.

The results of the investigation are shown in *Fig. 7*. As can be seen from this, the load-carrying capacity of the connections increases with a higher tensile strength of the filler materials. For each welding consumable used, the results show a small scatter with standard deviations between 9 and

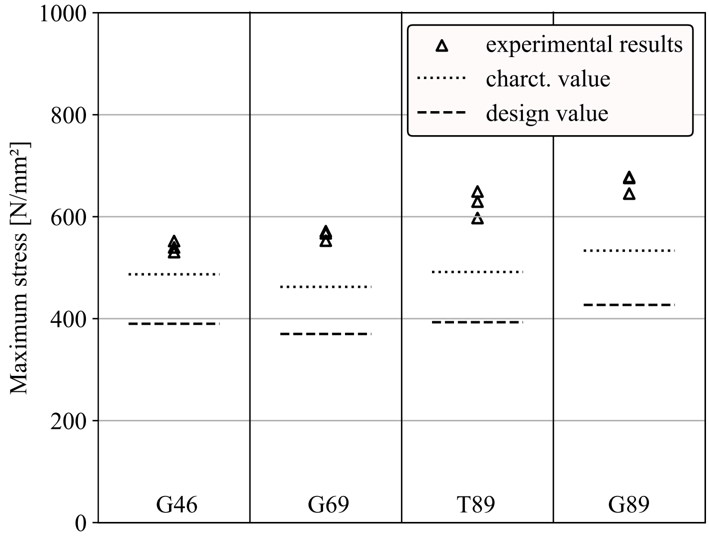

Fig. 7. Experimental results of ultra-high strength fillet welds dependent on the filler material used

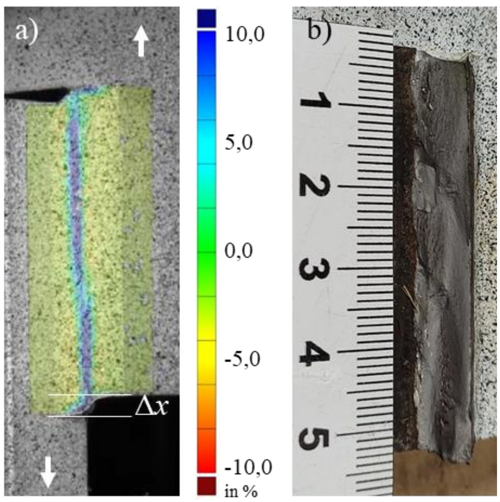

Fig. 8. Fillet weld with G46 a) deformation behaviour with ARAMIS, b) fracture surface

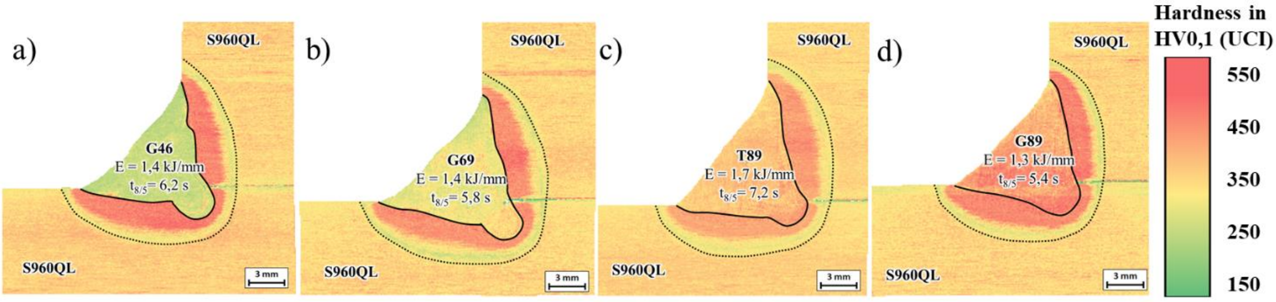

Fig. 9. Hardness mappings with UCI method of fillet welds on S960QL, t = 20 mm, made with a) G46, b) G69, c) T89 and d) G89

21 MPa. For comparison, the characteristic values (without γ_{M2}) and the design values (with γ_{M2}) from *Eq. (3)* are shown in *Fig. 7*. This demonstrates that the design concept currently valid up to S700 provides safe results for both matched and overmatched connections made out of S960.

The failure of all fillet welds occurred in the weld metal, with an average failure angle of approximately 45°. *Fig. 8* shows the deformation behaviour measured with ARAMIS and the fracture surface after failure of the specimen. The deformation behaviour is similar for all welding consumables used, with a fracture propagation in the middle of the fillet weld and displacements Δx of approximately 2,0 to 4,0 mm. There is a recognisable tendency for higher-strength filler materials to result in smaller deformation.

The hardness mappings in *Fig. 9* clearly show the increasing hardness with higher strengths of the filler material. Within the HAZ, similar behaviour can be seen for all filler materials regardless of their strength. There is an increase hardness value near the fusion line in the HAZ, while a soft zone is formed adjoining. Relatively homogeneous hardness values are observed in the weld metal region.

5 DESIGN CONCEPTS FOR ULTRA-HIGH STRENGTH WELDED JOINTS

5.1 General

Based on the results achieved, design concepts for butt welds and fillet welds were derived for steels S700 < S ≤ S960. The design concepts were already proposed in a CEN/TC 250/SC 3/WG 12 meeting for prEN 1993-1-12 (1). The objective was to extend the existing design concepts up to S960 to enable a safe and user-friendly design with UHSS. A detailed derivation and statistical evaluation of the design concepts is given in (16).

5.2 Butt welds

UHSS up to S960 will be included in the new generation of standards by prEN 1993-1-12 (1). A design equation was developed for FprEN 1993-1-8 (8) and is valid for HSS up to S700. In order to extend the design concept up to S960, the load-carrying capacity achieved in the experimental tests were statistically analysed in accordance with EN 1990, Annex D (17). It became apparent that an adjustment of the design equation *Eq. (1)* for butt welds with undermatching filler material is needed. Whereas the evaluation shows that the design concepts according to *Eq. (1)* for matching connections of S960 leads to reliable design results. In order to obtain an economical design model, it is therefore only necessary to adapt the equation for undermatching filler materials. For this purpose, a new coefficient β_U is introduced, the "U" referring to "Undermatching". Further evaluation showed that a reduction by $\beta_U = 1{,}05$ is sufficient to enable a safe design for undermatching butt-welded connections made of UHSS. Consequently, the design proposal for butt-welded connections of S700 < S ≤ S960 and different filler materials is as follows, see *Eq. (4)*.

$$\sigma_{\mathrm{v,Rd}} = \frac{0{,}85\ (0{,}9 f_{\mathrm{u}}) + 0{,}15 f_{\mathrm{u,FM}}}{\beta_U \gamma_{\mathrm{M2}}} \tag{4}$$

with:

β_{U} = 1,00 for matching filler material

β_{U} = 1,05 for undermatching filler material

Eq. (4) was also statistically analysed according to EN 1990, Annex D (17), resulting in the new design concept being on the safe side. Therefore, the proposed design concept enables a safe, user-friendly and economical design of butt welds made of UHSS with matching and undermatching filler material.

5.3 Fillet welds

There are two different design concepts for fillet welds, that are to be extended for S700 < S ≤ S960. In the case of undermatching joints, *Eq. (3)* is used, where the modified correlation coefficient depends entirely on the weld metal. The applicability of this design concept must be verified accordingly for UHSS. The test results were analysed and showed that *Eq. (3)* is on the safe side for undermatching UHSS connections. As a result, the design concept can be applied for S700 < S ≤ S960 and undermatching filler materials without adaption.

For matching connections, *Eq. (2)* should be used and a new correlation coefficient needed to be determined as part of the extension up to S960. Therefore, the results obtained from matching connections were investigated. Thus, the correlation coefficient β_{w} was determined to be 1,19 for S700 < S ≤ S960. The extension of the design proposals up to S960 enable simple, user-friendly and safe dimension of fillet welds made of UHSS.

6 SUMMARY

The load-carrying capacity and deformation behaviour of ultra-high strength butt- and fillet-welded joints made of S960 were investigated here. For this purpose, quasi-static tensile tests were carried out on the welded joints and both the stresses and strains were measured during testing. In addition, extensive material testing and hardness mappings with the UCI method were carried out on the specimens. The results obtained were used to formulate design recommendations for welded joints made of UHSS. Design concepts were developed for butt welds with undermatching or matching filler material and for fillet welds with matching and fillet welds with undermatching filler material, that were already presented to CEN/TC 250/SC 3/WG 12 for prEN 1993-1-12 (1). The design concepts developed can be used for steels S700 < S ≤ S960 and enable a safe and user-friendly design of welded joints.

7 ACKNOWLEDGEMENT

The IGF project "Effective design concepts for welded mixed connections in steel structures" (21412 BG/P 1507) of the Research Association for Steel Application e. V. (FOSTA), Sohnstraße 65, 40237 Düsseldorf, Germany, is a sub-project of the FOSTA joint research program HOCHFEST and was funded by the Federal Ministry for Economic Affairs and Climate Action via the AiF within the framework of the programme for the promotion of joint industrial research and development (IGF) on the basis of a resolution of the German Bundestag. Special thanks go to the industrial partners of the project committee for their support of the research project.

REFERENCES

1. **CEN/TC 250/SC 3/WG 12 N 139.** prEN 1993-1-12: Eurocode 3 - Design of steel structures - Part 1-12: Additional rules for steel grades up to S960. Brussels : European Committee for Standardization, working draft (unpublished), 2023.

2. **Kuhlmann, Ulrike, et al.** *Effiziente Nachweiskonzepte für Mischverbindungen im Stahlbau (engl. Effective design concepts for mixed connections in steel structures), Final report.* Düsseldorf : German Federation of Industrial Research Associations (AiF), in preparation. IGF: 21412 BG; FOSTA: P 1507.
3. **von Arnim, Mareike, et al.** Study on load-carrying capacity of MAG butt welded mixed connections with different steel strengths. *ce papers.* 3-4, 2023, Vol. 6, pp. 1458-1463.
4. **Eichler, Stefan, et al.** Heat management and tensile strength of 3 mm mixed and matched connections of butt joints of S355J2+N, S460MC and S700MC. *ce papers.* 3-4, 2023, Vol. 6, pp. 1479-1482.
5. **Amraei, Mohsen, et al.** Effects of heat input on the mechanical properties of butt-welded high and ultra-high strength steels. *Engineering Structures.* 198, 2019.
6. **Maurer, Wilhelm, et al.** Einfluss der Weichen Zone auf die mechanischen Eigenschaften hochfester Schweißverbindungen (engl. Influence of the soft zone on the mechanical properties of high-strength welded joints). *Schweiss-&Prüftechnik.* 2013, 10-15.
7. **Bergmann, Jean Pierre, et al.** *Tragfähigkeit von Stumpfnähten höherfester Stähle im Stahlbau (engl. Load-carrying capacity of butt welds of high strength steels in steel construction).* Düsseldorf : German Federation of Industrial Research Associations (AiF), 2020. IGF: 19.470 BG.
8. **FprEN 1993-1-8.** Eurocode 3: Design of steel structures - Part 1-8: Design of joints. *Formal vote version.* Brussels : European Committee for Standardization, 2023.
9. **Maurer, Wilhelm.** *Untersuchung der Auswirkung einer Weichen Zone auf die Festigkeitseigenschaften von hochfesten Schweißverbindungen (engl. Investigation of the effect of a soft zone on the strength properties of high-strength welded joints).* Graz University of Technology : Dissertation, 2014.
10. **Schaupp, Thomas, et al.** Welding residual stresses in 960 MPa grade QT and TMCP high-strength steels. *Journal of Manufacturing Processes.* 27, 2017, pp. 226-232.
11. **Brätz, Oliver, et al.** Load-carrying capacity of MAG butt and fillet welded joints on high-strength structural steels of grade S960QL and S960MC. *ce papers.* 3-4, 2023, Vol. 6, pp. 587-594.
12. **EN ISO 6892-1.** Metallic materials - Tensile testing - Part 1: Method of test at room temperature. Brussels : European Committee of Standardization, 2019.
13. **ASTM A 1038.** Standard Test Method for Portable Hardness Testing by the Ultrasonic Contact Method. : American Society for Testing and Materials, 2019.
14. **DIN 50159-1.** Metallische Werkstoffe - Härteprüfung nach dem UCI-Verfahren - Teil 1: Prüfverfahren. Berlin : Beuth Verlag GmbH, 2022.
15. **von Arnim, Mareike, et al.** Effiziente Nachweiskonzepte für geschweißte Mischverbindungen im Stahlbau (engl. Effective design concepts for welded mixed connections in steel structures). *Stahlbau.* 91, 10, 2022, pp. 660-670.
16. **von Arnim, Mareike.** *Tragfähigkeit und Verformungsverhalten von hochfesten Schweißverbindungen bis S960 (engl. Load-carrying capacity and deformation behaviour of high strength welded joints up to S960).* University of Stuttgart, Institute of Structural Design : Dissertation, in preparation.
17. **EN 1990.** Eurocode: Basis of structural design. Brussels : European Committee for Standardization, 2010.